Self-assembled poloxamer-legumin/vicilin nanoparticles for the nanoencapsulation and controlled release of folic acid

Fang, Changhao; Kanemaru, Karen; Carvalho, Wildemar S.P.; Fruehauf, Krista R.; Zhang, Sunshine; Das, Prem P.; Xu, Caishuang; Lu, Yuping; Rajagopalan, Nandhakishore; Kulka, Marianna; Makeiff, Darren A.; Serpe, Michael J.

Publisher's version / Version de l'éditeur:
https://doi.org/10.1016/j.ijbiomac.2024.131646
International Journal of Biological Macromolecules, 268, P2, 2024-04-16

International Journal of Biological Macromolecules 268 (2024) 131646

Contents lists available at ScienceDirect

International Journal of Biological Macromolecules

journal homepage: www.elsevier.com/locate/ijbiomac

Self-assembled poloxamer-legumin/vicilin nanoparticles for the nanoencapsulation and controlled release of folic acid

Changhao Fang [a], Karen Kanemaru [a], Wildemar S.P. Carvalho [a], Krista R. Fruehauf [a], Sunshine Zhang [a], Prem P. Das [d], Caishuang Xu [d], Yuping Lu [d], Nandhakishore Rajagopalan [d,e], Marianna Kulka [b,c], Darren A. Makeiff [b,*], Michael J. Serpe [a,*]

[a] Department of Chemistry, University of Alberta, Edmonton, AB T6G 2G2, Canada
[b] Quantum and Nanotechnologies Research Centre, National Research Council Canada, 11421 Saskatchewan Dr NW, Edmonton, AB T6G 2M9, Canada
[c] Department of Medical Microbiology and Immunology, University of Alberta, Edmonton, AB T6G 2G2, Canada
[d] Aquatic and Crop Resource Development Research Centre, National Research Council Canada, 110 Gymnasium Pl, Saskatoon, SK S7N 0W9, Canada
[e] Department of Chemical and Biological Engineering, University of Saskatchewan, 57 Campus Drive, Saskatoon, SK S7N 5A9, Canada

ARTICLE INFO

Keywords:
Nanoencapsulation
Legumin and vicilin
Fava beans
Folic acid
Drug delivery
Self-assembly

ABSTRACT

Plant-based food proteins are a promising choice for the preparation of nanoparticles (NPs) due to their high digestibility, low cost, and ability to interact with various compounds and nutrients. Moreover, nanoencapsulation offers a potential solution for protecting nutrients during processing and enhancing their bioavailability. This study aimed to develop and evaluate nanoparticles (NPs) based on legumin/vicilin (LV) proteins extracted from fava beans, with the goal of encapsulating and delivering a model nutraceutical compound, folic acid (FA). Specifically, NPs were self-assembled from LV proteins extracted from commercially available frozen fava beans using a pH-coacervation method with poloxamer 188 (P188) and chemically cross-linked with glutaraldehyde. Microscopy and spectroscopy studies were carried out on the empty and FA-loaded NPs in order to evaluate the particle morphology, size, size distribution, composition, mechanism of formation, impact of FA loading and release behavior. In vitro studies with Caco-2 cells also confirmed that the empty and FA-loaded nanoparticles were non-toxic. Thus, the LV-NPs are good candidates as food additives for the delivery and stabilization of nutrients as well as in drug delivery for the controlled release of therapeutics.

1. Introduction

Recent technological advances have significantly augmented the nutritional profile and bioactive attributes of food and nutrient supplementation products. Despite these advances, traditional methods such as food fortification and tablet-based supplementation persist as the predominant approaches employed in the development of functional foods and dietary supplements. While traditional food fortification-based and tablet-based supplementation methods have many benefits, nanoparticle-based strategies have emerged as a promising approach for encapsulating and delivering therapeutics and nutraceuticals [1]. The encapsulation of bioactive molecules within nanoparticles provides numerous benefits, including protection from degradation, improved water solubility, and enhanced bioavailability [2,3]. Various materials, such as natural and synthetic polymers as well as inorganic compounds, have been used to develop nanoparticles suitable for encapsulating a wide range of therapeutics and nutraceuticals. Moreover, nanoparticle-based delivery systems allow for stimuli-responsive, targeted and sustained release of encapsulated molecules, which can lead to improved therapeutic outcomes [4]. Due to these benefits, nanoparticles-based strategies have shown great potential in fields such as medicine, agriculture, and food science.

Folic acid (FA), also known as vitamin B9, is an essential vitamin in the human diet obtained through the consumption of green vegetables or dietary supplements [5]. FA is involved in processes such as DNA, RNA, and amino acid metabolism, which are necessary for rapid cell division and growth, especially during pregnancy and infancy [5]. FA deficiency can lead to a variety of complications and diseases such as anemia [6], Alzheimer's disease [7], and cancer [8]. Common methods employed to reduce the risks associated with FA deficiency and increase daily uptake include the fortification of foods (flour, bread, milk, etc.) and tablet-based supplements with FA [9]. However, FA and folates are

* Corresponding authors.
E-mail addresses: Darren.Makeiff@nrc-cnrc.gc.ca (D.A. Makeiff), serpe@ualberta.ca (M.J. Serpe).

https://doi.org/10.1016/j.ijbiomac.2024.131646
Received 2 January 2024; Received in revised form 12 April 2024; Accepted 14 April 2024
Available online 16 April 2024

sensitive to temperature, pH, light, oxidation and other changes in environmental conditions, which can facilitate the conversion into biologically inactive forms [10]. Therefore, there is a need to develop carrier-mediated transport systems in order to improve the absorption of FA as well as its bioavailability.

Nanoencapsulation has also been used to address the instability of FA [11]. The chemical decomposition of encapsulated FA during food processing and cooking may be inhibited while the oral bioavailability is improved [12]. Strategies for the nanoencapsulation of FA include electrospinning [13], oil/water emulsions [14], nanogels [15], inorganic nanoparticles (NPs) [16] and naturally-derived proteins [12], each of which has pros and cons. As a promising nanoencapsulation strategy, protein NPs offer great nutritional value, are easy to obtain from natural sources, are relatively inexpensive and have excellent biodegradability, biostability and biocompatibility [17] [18].

Plant-based proteins have attracted significant attention recently due to their advantages over animal-based proteins: larger variety of sources, lower cost, improved safety (lower immunogenicity) and suitability for vegetarian food preferences [19,20]. Examples of plant-based proteins include gliadin, zein, legumin, and vicilin [18]. Main globulin storage proteins present in leguminous seeds including beans, peas and lentils, legumin and vicilin (LV) proteins have attracted much attention due to their widespread availability, high digestibility, and versatile functional properties [21,22]. In fava bean (*Vicia faba L.*), which is one valuable source of plant-based proteins popular in many countries from the Middle East, the Mediterranean region, South America and East Asia [23], legumin (11S fraction) accounts for 40–45 % of total proteins with a hexameric native form and a molecular weight of 340–400 kDa [24]. On the other hand, vicilin (7S fraction) accounts for 20–25 % of total proteins and has a trimeric native form and a molecular weight of 160–200 kDa [25].

The distinctive structural and physicochemical properties of LV proteins render them particularly intriguing for the design of nanoparticle-based encapsulation and delivery systems [22]. For example, nanoparticles from LV proteins isolated from peas (*Pisum sativum* L.) were first reported in the mid-late 1990's with the first report of legumin NPs by Irache et al. [26] and later vicilin NPs by Ezpeleta et al. [27,28]. However, owing to their unique structural and physicochemical properties, LV proteins exhibit poor solubility in water [29], which makes them well-suited for encapsulating hydrophobic compounds like resveratrol [30] but less suitable for hydrophilic compounds or nutrients. To overcome this limitation, Guo et al. utilized surfactants to complex LV-rich pea protein isolates, thereby enhancing solubility for curcumin encapsulation [19]. Yet, to the best of our knowledge, no other reports exist on the use of LV protein-based NPs to encapsulate other pharmaceutical/nutraceuticals, let alone FA. Hence, there is a pressing need for the development of novel methodologies to modify the functional properties of LV proteins to facilitate the encapsulation and release of hydrophilic compounds or nutrients, such as FA.

The objective of this study was to extract and functionalize fava bean LV proteins to prepare nanoparticles as nanocarriers for the important nutrient FA. For this purpose, commercial fava beans from the local market were used as a source to isolate LV proteins using the isoelectric precipitation method [31], followed by pH-coacervation self-assembly to prepare LV-NPs, stabilized by a surfactant, and then hardened via glutaraldehyde cross-linking. The characteristics of these NPs, spectroscopic properties and morphology/nanostructure as well as the encapsulation of FA, encapsulation efficiency, loading capacity and release profiles under different conditions were examined. Also, cytotoxicity studies with Caco-2 cells were also carried out. This research presents a detailed strategy for purifying and characterizing LV proteins from commercially available fava beans. We utilized these proteins to develop FA-encapsulating NPs through P188 stabilization and GA-hardened self-assembly. Additionally, we investigated the release profile of folic acid under various conditions. Our findings offer valuable insights and applications for both academic research and industry practices in food chemistry and pharmaceutical delivery.

2. Materials and methods

2.1. Materials

Frozen fava beans were obtained from a local grocery store (Tong Sheng, T & T Supermarket, Edmonton, AB, Canada). AlamarBlue reagent was obtained from Bio-Rad Laboratories, Inc. (Mississauga, ON, Canada). Caco-2 cells (HTB-37™) were purchased from the American Type Culture Collection (ATCC) (Manassas, VA, USA). TrypLE™ Express Enzyme (1×), phenol-red free Eagle's Minimum Essential Medium (EMEM), fetal calf serum and 1 % penicillin/streptomycin solution were obtained from Thermo Fisher Scientific (Waltham, MA USA). All other chemicals, including phosphate buffer saline (PBS), poloxamer 188 (P188), 50 % glutaraldehyde (GA), 8-anilino-1-naphthalenesulfonic acid (ANS), folic acid (FA), pepsin, and pancreatin, were purchased from Sigma-Aldrich (Oakville, ON, Canada) and used as received. Simulated gastric fluid (SGF) and simulated intestinal fluid (SIF) were prepared according to United States Pharmacopoeia 2020 (USP 43-NF 38). Deionized (DI) H_2O was obtained from MilliporeSigma™ Milli-Q™ Direct Water Purification System.

2.2. Preparation of samples

2.2.1. Pre-treatment of frozen fava bean

The pre-treatment procedure of frozen fava beans is illustrated in Scheme 1. Frozen fava beans (454 g) were thawed by soaking in 2 L distilled water (dH_2O) at 4 °C for 24 h. Afterward, the fava beans were dehulled manually to remove the shell component. The fava bean seeds were then dried under constant natural airflow in a fume hood for 48 h, before being ground into powder using a coffee grinder (Black & Decker, CBG100SC). The resulting fava bean powder (100 g) was defatted with isopropanol (300 mL) by dispersing the powder in isopropanol for 1 h with stirring (600 RPM) and then filtered three times, and dried in vacuo for 48 h.

2.2.2. Isolation of legumin/vicilin from fava bean powder via isoelectric precipitation

The procedure used for isolating LV was similar to previous literature report (Zhao, [19,31]) but at a smaller scale. In a typical experiment,

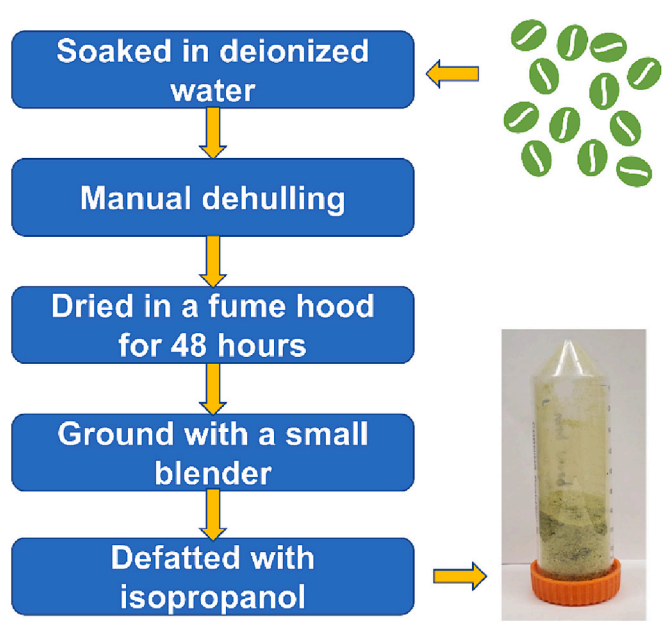

Scheme 1. Pre-treatment of frozen fava beans

fava bean powder (10 g) was mixed with dH_2O (90 mL). The pH was adjusted to ~9 using 1 M NaOH and the mixture was stirred at 50 °C. After 1 h, the suspended solid was collected by centrifugation (5000 *g*, 20 min) and the supernatant was decanted. NaCl (1.8 g) was then added to the supernatant to give a concentration of 0.5 M, and the pH was adjusted to 4.8 with 1 M HCl to yield a precipitate. The precipitated proteins were collected by centrifugation (5000 *g*, 20 min) and the supernatant was decanted away. The supernatant was then diluted with DI H_2O (20 mL) until the concentration of NaCl was 0.3 M to yield another precipitate, which was collected by centrifugation (1000 *g*, 20 min). The supernatant was removed, and the pelletized solid was then redispersed in 0.6 M NaCl (20 mL). The mixture was then centrifuged (5000 *g*, 20 min) again and the supernatant was decanted away from the pelletized solid and diluted with the same volume of DI H_2O. After 4 h at 23 °C, the supernatant was carefully decanted from the settled precipitates that had formed. The resulting solid purified proteins were then solubilized in dH_2O (10 mL) after the pH was adjusted to 7.2 with 1 M NaOH. This solution was then dialyzed (20 kDa MWCO) against DI H_2O at 4 °C for 40 h, frozen with liquid nitrogen and then freeze-dried for 48 h to obtain a white powder (134.4 ± 38.8 mg, 1.3 ± 0.4 %).

2.2.3. Synthesis of legumin/vicilin nanoparticles (LV-NPs)

This process was adapted from a procedure that was previously reported. [26,32]. Briefly, purified protein powder (15 mg) was dissolved in DI H_2O (3 mL) at pH = 11 and 80 °C with stirring at 500 RPM. After 20 min, a solution of 0.2 % P188 in PBS buffer (6 mL, pH = 6.8) was added and the mixture was heated at 80 °C for additional 10 min. Then, 50 % GA solution (3 μL) of was added to induce protein cross-linking. The reaction was then cooled to 22 °C. After 2 h of stirring at 500 RPM, the suspended solid was collected by centrifugation (5000 *g*, 15 min) using a Amicon® Ultra-15 Centrifugal Filter Unit (30 KDa MWCO). The filtrate was discarded, and the residue was washed several times with fresh PBS (15 mL × 3, pH = 7.4) and then DI H_2O (15 mL × 3). The LV-NPs were then dispersed in DI H_2O and stored at 4 °C for future experiments.

2.2.4. Synthesis of folic acid-loaded legumin/vicilin nanoparticles (FA-LV-NPs)

FA loaded LV-NPs were synthesized using a similar procedure to synthesize empty LV-NPs (Scheme 2). In a typical experiment, purified protein powder (15 mg) was dissolved in 1 mg/mL FA solution (3 mL) at pH = 11 and 80 °C. After 20 min, 0.2 % P188 in PBS (6 mL, pH = 6.8) was added and the mixture was heated at 80 °C for additional 10 min. Then, 50 % GA solution (3 μL) of was added to induce protein cross-linking. The reaction was then cooled to room temperature. After 2 h, the suspended solid was collected by centrifugation (5000 *g*, 15 min) using a Amicon® Ultra-15 Centrifugal Filter Unit (30 KDa MWCO). The filtrate was discarded and the residue was washed several times with fresh PBS (15 mL × 3, pH = 7.4) followed by DI H_2O (15 mL × 3). The FA-L*V*-NPs were then dispersed in DI H_2O and stored at 4 °C for future experiments.

2.2.5. Determination of the encapsulation efficiency and loading capacity of FA in FA-LV-NPs

The amount of encapsulated FA was determined by incubating the sample in SGF at 37 °C for 24 h to decompose proteins as much as possible, followed by ultracentrifugation to extract the released FA. The concentration of released FA was quantified via fluorescence spectroscopy by using a calibration curve of FA in SGF. The encapsulation efficiency (EE) was calculated according to the following equation:

$$\mathrm{EE}\ (\%) = \frac{\text{encapsulated FA}}{\text{total FA input}} \times 100$$

The EE was measured to be 13.5 ± 1.4 %.

2.3. Characterization

2.3.1. Electrophoresis

Sodium dodecyl sulfate-polyacrylamide gel electrophoresis (SDS-PAGE) was performed using a 12 % acrylamide resolving gel and a 5 % acrylamide stacking gel. Approximately 10 μg of each sample was loaded per well and 10 μL of Bluelf Prestained Protein Ladder (Froggabio, Vaughan, Ontario, Canada) was used as the protein ladder. The electrophoresis was run at 80 V for 20 min and 120 V for 1 h. To detect the proteins, the gel was stained with 1 mg/mL Coomassie Brilliant Blue R250 solution for 18 h and then destained using 6:3:1 DI H_2O:methanol: acetic acid over 4 h.

2.3.2. Sample preparation and shotgun mass spectrometry (LC-MS/MS)

Dried fava bean isolate (10 mg) was reconstituted in a buffer containing triethylammonium bicarbonate (TEAB) and 5 % sodium dodecyl sulfate (SDS) at pH 8. The sample was vigorously mixed and incubated at room temperature for 15 min before centrifugation (12,000 rpm, 10 min). As a quality control step, before proceeding to trypsin digestion, the collected supernatant was subjected to SDS-PAGE analysis. Subsequently, S-Trap™ (Protifi) column -based trypsin digestion of sample was performed according to manufacturer's recommendations. To ensure equal loading of peptide sample for mass spectrometry, Pierce™ Quantitative Colorimetric Peptide Assay (Thermo Scientific™) was utilized according to manufacturer's protocol to quantitate total peptide in sample. Digested peptide sample was again used for SDS-PAGE analysis to confirm the complete digestion of the proteins. A total amount of 100 μg of peptide sample was freeze-dried and redissolved with 75 μL of 5 % acetonitrile solvent.

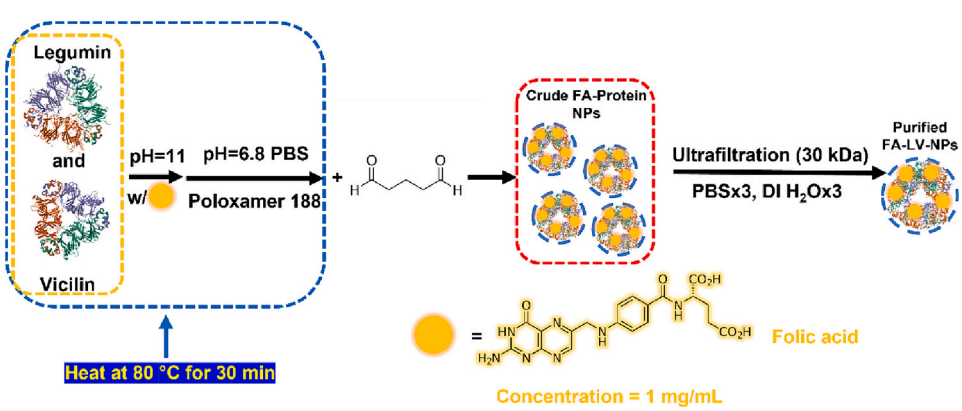

Scheme 2. Synthesis of FA-LV-NPs

Two technical replicates of 25 μg each of digested peptide sample were injected into Vanquish UHPLC system (Thermo Scientific™) coupled to a Thermo Scientific™ Q Exactive™ mass spectrometer. The Liquid Chromatography (LC) system was connected to a reverse phase C18 Acclaim™ RSLC C18 (1 × 150 mm, 2.2 μm, Thermo Scientific™) column coupled with guard cartridge Pepmap100 C18 (11 × 5 mm, 5 μm, Thermo Scientific™) and the column was maintained at 60 °C. The LC-MS/MS data was collected in data dependent acquisition (DDA) mode. Using a flow rate of 50 μL/min, mobile phase A (0.1 % formic acid in water) and phase B (0.1 % formic acid in 80 % acetonitrile with water) were mixed to generate the following gradient: 4–40 % phase B in 83 min, 40–65 % phase B in next 5 min, 65–100 % phase B in 2 min, hold at 100 % phase B for 10 min, then back to 4 % phase B for 1 min before equilibrating the column at 4 % phase B for 20 min. Eluted peptide samples were ionized by electrospray ionization (ESI) source, injected into the MS and data acquired using Full MS/dd-MS^2. The following parameters were set to acquire Full MS data: resolution 70,000, precursor ion scan range 375–1800 *m/z*, AGC target 3e6 and accumulation time of 100 ms in positive ion mode at 2 default charge. For subsequent MS/MS analysis, the top 12 most abundant precursors in each duty cycle were selected for data-dependent MS/MS fragmentation with resolution at 17,500, AGC target at 2e5, accumulation time 220 ms, loop count 12, isolation window 1.6 m/z, normalized collision energy (NCE) 30 and dynamic exclusion of 30 s.

After collecting of raw data file, PEAKS Studio 10.6 (build 20,201,221) software was used for protein identification. For protein identification, MS2 spectra were searched against FASTA sequences of Fava bean (*Vicia faba*) database downloaded from uniport server and coupled with common contaminants (cRAP) database. The software uses predefined database search workflow with default setting as follows: Parent Mass Error Tolerance: 10.0 ppm, Fragment Mass Error Tolerance: 0.05 Da, modification search off and FDR: 1 %.

2.3.3. Dynamic light scattering (DLS)

The hydrodynamic diameter (D_h in nm) and polydispersity index (PDI) were measured using a Nano ZS90 Malvern Zetasizer (Malvern Instruments, Worcestershire, UK) equipped with a light source with a wavelength of 633 nm. The light scattering intensity was detected at 173°.

2.3.4. Transmission electron microscopy (TEM)

The size and morphology of the protein and protein nanoparticle samples were examined using a JEM-ARM200 Atomic Resolution S/TEM (JEOL Ltd., Tokyo, Japan). TEM samples were prepared by placing a drop of dispersion of solutions on a carbon film-coated copper grid (CF400-CU, Electron Microscopy Sciences, USA). The samples were dried before image acquisition.

2.3.5. Spectroscopy

Ultraviolet-Visible (UV–Vis) spectra were acquired using a Hewlett Packard 8453 UV–Vis Spectrophotometer (Santa Clara, CA, USA). Fourier-transform infrared (FTIR) spectra were acquired using a Thermo Nicolet 8700 FTIR spectrometer (Waltham, MA, USA). The powder samples were mixed with KBr to form a pellet for FTIR analysis. Fluorescence emission spectra were acquired using a Horiba-PTI QM-8075-11 Fluorescence System (Kyoto, Kyoto, Japan). Circular dichroism (CD) spectra were recorded on an Olis DSM 17 Circular Dichroism spectrometer (Athens, GA, USA). The secondary structure content was calculated on-line using DichroWeb [33].

2.3.6. Surface hydrophobicity (H_0) assay

H_0 was determined using the assay based on the fluorescent dye 8-anilino-1-naphthalenesulfonic acid (ANS) according to literature [34]. Three different samples: LV, LV-NPs and FA-LV-NP powders (0.2–1 mg/mL) were dispersed in water at pH = 11. Then, 10 μL of ANS (8 mM, pH = 11) was mixed with 500 μL of the sample. The fluorescence of the samples was measured in a 96-well plate with a SpectraMax i3x plate reader using an excitation wavelength of 375 nm and emission wavelength of 470 nm. Finally, the H_0 values were acquired by determining the slope of fluorescence intensity vs. protein concentration.

2.4. Folic acid release study

The release of FA was examined under two different simulated conditions using simulated gastric fluid (SGF) and simulated intestinal fluid (SIF) both with and without the enzymes pepsin and pancreatin, respectively. For SGF with pepsin, pepsin (2500 units/mg protein) was added at a concentration of 3.2 mg/mL. For SIF with pancreatin, pancreatin was added at a concentration of 6.8 mg/mL. The enzymes were added during the preparation of the media and the media were immediately used for the release study. A 250 μL aliquot of FA-LV-NPs dispersed in DI H_2O (25 mg/mL) was added to either SGF or SIF (1 mL) and incubated at 37 °C for a total of 2 h in SGF and 6 h in SIF. At different times, an aliquot (500 μL out of the total 1.25 mL) was removed and filtered using Amicon® Ultra-0.5 Centrifugal Filter Units (3 KDa) and an Eppendorf Centrifuge 5420 (21,300 *g*, 5 min). The resulting filtrate (300 μL) was collected. The filtered solid was redispersed in 300 μL of fresh simulated fluid and returned to the original 1.25 mL mixture. The collected fractions (300 μL filtrate) were places into a 96-well plate and the fluorescence of samples was measured with a SpectraMax i3x plate reader. Excitation and emission wavelengths 420 nm and 460 nm respectively were used to determine the FA concentration in SGF (Fig. S5). For the measurements in SIF, an excitation and emission wavelengths of 395 nm and 450 nm were used, respectively (Fig. S6).

2.5. In vitro cell viability assay

2.5.1. Caco-2 cell culture

Caco-2 cells were cultured in phenol-red free, Eagle's Minimum Essential Medium (EMEM) containing 10 % fetal calf serum and 1 % penicillin/streptomycin at 37 °C in a humidified atmosphere with 5 % CO2. Caco-2 grown in T-75 flasks were passaged using TrypLE™ Express Enzyme (1×) when they reached 80 % confluency. The growth medium was changed every 2 days, and the cells were passaged every week. The Caco-2 cells at passage 3 were used for further experiments.

2.5.2. Cell viability assay

AlamarBlue assay was used to measure the metabolic activity of the Caco-2 cells following treatment with the different samples: LV proteins, LV-NPs, and FA-LV-NPs toward Caco-2 cells. In detail, Caco-2 cells were seeded in 24-well plates in complete medium (0.5 mL) at a density of 30,000 cells/well and cultured in 5 % CO_2 at 37 °C for 24 h so that the cells could adhere to the plates. Then different concentrations of LV-NPs, and FA-LV-NPs were added to the growth medium and incubated. After incubation for 24 or 96 h, the medium was removed and the cells were washed with sterile PBS (137 mM NaCl, 2.7 mM KCl, 10 mM Na_2HPO_4, and 1.8 mM KH_2PO_4) once, followed by the addition of fresh medium containing 10 % *v*/v of alamarBlue reagent (Bio-Rad Laboratories, Inc., Mississauga, ON, Canada), the weakly fluorescent resazurin dye which undergoes reduction to resorufin which is highly fluorescent. The cells and dye mixture were then further incubated at 37 °C. After 4 h, 100 μL of the supernatant was removed from each well, transferred to a 96-well plate and the fluorescence emission of resorufin was measured at 590 nm (excitation = 560 nm) using a SpectraMax i3x plate reader. Caco-2 cells cultured in a growth medium without any treatment were used as the control. The reduction of the resazurin dye was expressed as a percentage of the cell viability for the experiment compared to the control.

$$\text{Cell Viability } (\%) = \frac{\text{FL intensity of alamarBlue assay of experimental groups}}{\text{FL intensity of alamarBlue assay of control groups}} \times 100$$

3. Results and discussion

3.1. Isolation of legumin/vicilin from fava beans

A multi-step purification process was carried out obtain pure LV isolate from grocery store-bought frozen fava beans for the formation of the NPs. The first step involved removal of most of the fiber and fat content, leaving the protein-rich flour (Scheme 1). Next, the fava bean flour was subjected to a modified isoelectric precipitation procedure. Fava bean flour was heated in an alkaline solution to extract most of the soluble proteins, including LV. Then, the pH was adjusted to 4.8, which is the isoelectric point of both LV [24,25,31,35], thus triggering the formation of precipitates that can be isolated via centrifugation. The product was then further purified by washing with salt solutions and dilution with water to yield a highly pure protein powder containing only LV. The final yield of LV protein isolate was 134.4 ± 38.8 mg from 10 g of fava bean flour.

The composition of the proteins isolated was determined using SDS-PAGE (Fig. S1) and mass spectrometry-based proteomics analysis (Table S1). The SDS-PAGE analysis showed the presence of abundant bands belonging to the vicilin subunits and legumin α and β chains (lane 1, Fig. S1). The results also revealed that the extraction procedure had enriched the LV proteins and removed most of the other seed storage proteins, such as, albumins and other lower molecular weight proteins. These extracted proteins were digested using trypsin and further proteomics studies were performed to confirm the identity of the peptides and proteins present in the sample. 21 proteins were identified (Table S1), most of which belong to the globulin protein families such as legumin, vicilin and convicilin. Furthermore, the ion peak area information was used to determine the relative abundance of these 21 proteins, which revealed that LV proteins comprise nearly 97 % of total the proteins present in the extract. These results are consistent with previous reports [31,35].

3.2. Synthesis of nanoparticles from LV

The LV-NPs were prepared using a pH coacervation method, similar to the procedure described by Mirshahi et al. [32,36]. First the LV protein isolate was dissolved in water at pH 11 at 80 °C, followed by the addition of the stabilizer P188 and cross-linking with glutaraldehyde. For LV-NPs loaded with FA, stabilization and cross-linking of LV was carried out in the presence of different amounts of FA. For an initial FA loading of 1 mg/mL, the encapsulation efficiency and loading capacity were measured to be 13.5 ± 1.4 % and 26.3 ± 2.8 mg/g, respectively.

3.3. Characterization of LV-NPs and FA-LV-NPs

3.3.1. Morphology and size measurements of nanoparticles

The hydrodynamic diameter of the LV isolates, LV-NPs and FA-LV-NPs were characterized by DLS. Multiple D_h's (i.e., 15 and 200 nm) and a very broad size distribution (i.e., PDI = 0.908 ± 0.149) were measured for the LV isolate in water (Fig. S2a), which was not surprising since LVs are each composed of different subunits, and the fast association/disassociation kinetics between the different subunits and/or proteins could also contribute to a broad distribution of various sized aggregates [37]. In contrast, DLS data (Fig. 1a) for the LV-NPs indicated a dispersion monodisperse particles (PDI value from 0.1 to 0.2) with an average D_h of 50–60 nm.

The morphology of the LV isolate and LV NPs was investigated by TEM. TEM images of the LV isolate did not show any evidence of any well-defined particles (Fig. S2b). In contrast, TEM images of LV-NPs (Fig. 1b) showed pseudo-spherical NPs, with a qualitative average diameter of 100 nm, which is consistent with the DLS data. Note that NPs <200 nm in size are beneficial as they are known to undergo receptor-mediated endocytosis into various cells [38], thus increasing the efficiency of NP uptake. Clearly, these results demonstrate that LV-NPs were successfully synthesized and the particle sizes are favorable for applications such as nutrient uptake (Fig. 1).

3.3.2. Spectroscopic characterization

UV–Vis and fluorescence spectroscopy were used to investigate the differences between LV isolates and formed LV-NPs. UV–Vis spectra of LV isolates and LV-NPs were similar (Fig. 2a and b), exhibiting absorbances at 210 nm and 280 nm, which correspond to electronic transitions from the peptide bond backbone and the presence of aromatic residues of phenylalanine, tryptophan, and tyrosine in the protein structure, respectively. Fluorescence emission spectra also further confirmed the presence of aromatic residues in both LV isolates and LV-NPs. Both materials exhibited emission peaks at 330 nm (λ_{ex} = 284 nm, typical for aromatic amino acids), which corresponds to the presence of aromatic residues. These results suggest that the LV isolates and NPs were indeed protein-based.

3.4. Mechanism of formation of LV-NPs

3.4.1. FTIR spectra

FTIR was used to examine the chemical composition and differences in the secondary structure of the LV isolates and LV-NPs. The spectrum for the LV-NPs exhibited signals at 1541, 1343, 1280, 1242, 1105, 962 and 842 cm^{-1}, which confirmed the presence of P188 (Fig. 3). Both of the FTIR spectra for LV isolates and LV-NPs showed C═O stretching bands in the amide I region at 1633 cm^{-1} and 1649 cm^{-1}, respectively. The shift to lower wavenumbers (~16 cm^{-1}) indicates that the C═O groups for the proteins in the LV isolate are involved in stronger hydrogen bonding interactions than the LV-NPs. Also, the position of the amide I bands are consistent with a predominantly β-sheet secondary structure (1625–1640 cm^{-1}) for the LV isolate and disordered structures (1640–1648 cm^{-1}) or α-helical secondary structure (1648–1660 cm^{-1}) for the LV-NPs [39]. β-sheet secondary structures are common for storage proteins such as legumin and vicilin from vegetal sources such as fava beans [25].

3.4.2. CD spectra

CD spectroscopy is a powerful tool to evaluate protein secondary structures involved in a variety of protein dynamics including protein folding, denaturation, and aggregation [40]. CD spectra of the LV isolate were recorded at 20 °C and 80 °C, in order to probe the effect of heating on the secondary structure of the proteins in the LV isolate during the NP formation. At 20 °C, the CD spectrum displayed a positive peak below 200 nm, the LV isolates showed a negative peak at 208 nm with a shoulder around 220 nm (Fig. 4a), which is consistent with a mixture of protein secondary structures, with β-sheet structures as the major components [41]. At 80 °C, both the positive and negative peaks shifted to 190 and 206 nm, respectively. The observed shift distinctly suggests a decrease in ordered structures and an increase in the random coil conformation, as suggested by Nivala et al. [42]. For the LV-NPs at 20 °C, a negative peak was observed at 204 nm which is blue-shifted by 2 nm relative to the LV isolate while the shoulder peak at 220 nm was

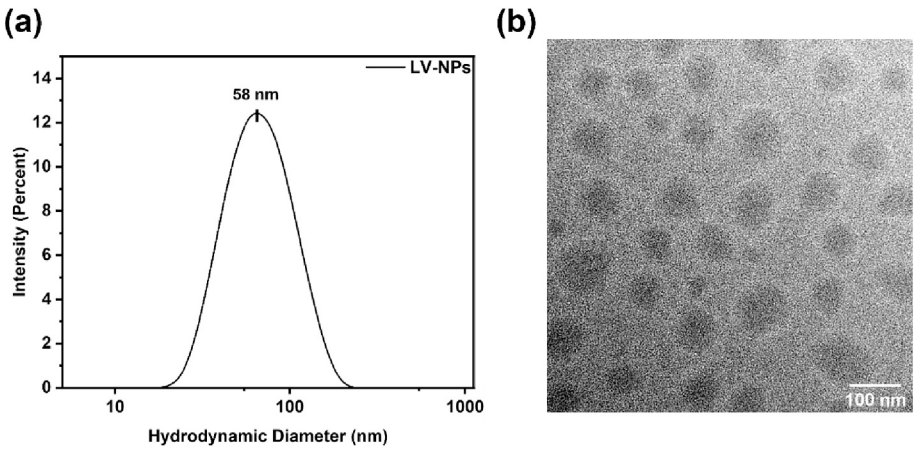

Fig. 1. Representative DLS measurements (a) and TEM images (b) of LV-NPs.

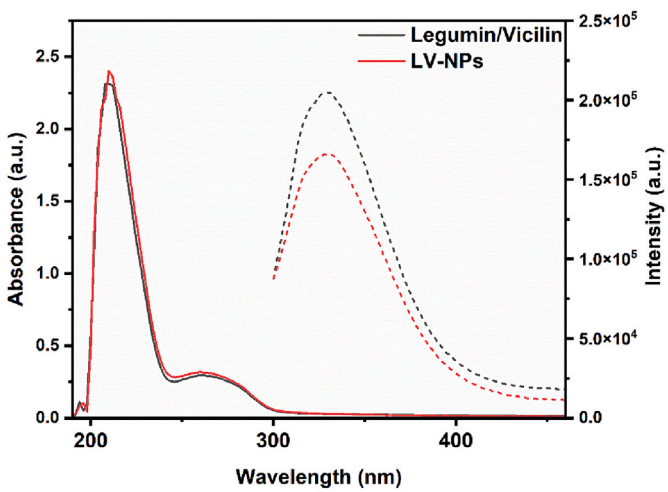

Fig. 2. UV–Vis spectra (solid lines) and fluorescence emission spectra (dashed lines) (λ_{ex} = 284 nm) of LV isolates and LV-NPs.

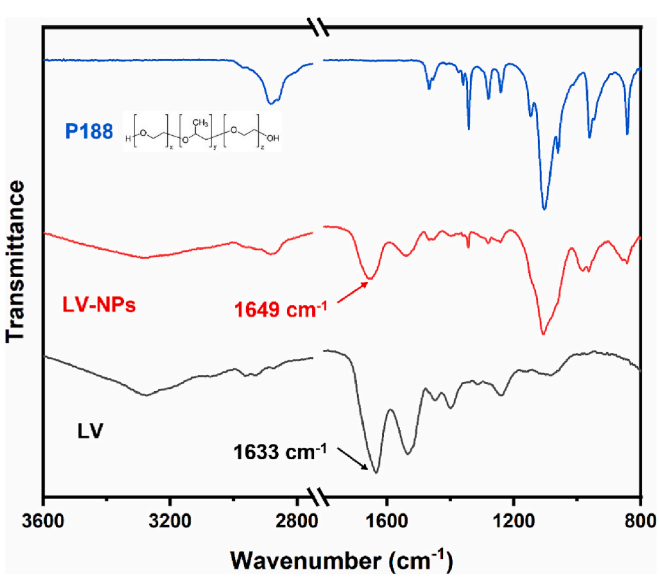

Fig. 3. FTIR spectra of P188, LV-NPs, and LV.

less apparent, which indicated major protein secondary structural changes relative to the LV isolate.

The secondary structure content of the LV isolate, denatured LV isolate at 80 °C and LV-NPs was calculated using DichroWeb analysis [33] of the CD data. The results are summarized in Fig. 4, which shows that the LV isolate at 20 °C had a combined β-structure (both sheet and turn) of 53 % and only 38 % of the proteins corresponded to a disordered region. Husband et al. observed similar characteristics in the secondary structure composition of their fava bean protein isolate that underwent purification through the isoelectric precipitation method [41]. Upon heating the LV isolate to 80 °C, the total β-structure portion decreased from 53 to 42 % while disordered structure increased from 38 to 53 %, indicating decreased ordered structure and increased random coil formation [42]. For the LV-NPs, the total β-structure content was similar to the LV isolate proteins at 80 °C, consisting of 52 % β-structure and 39 % disordered structure. These results are consistent with the denaturation of the origin LV isolate protein structure with heating, which is retained after cross-linking to form the LV-NPs. Furthermore, our results were notably different than those reported for traditional pea protein [43] and soy protein nanoparticles [44], in which the addition of $K_2S_2O_5$ or $CaCl_2$ enhanced the β-structure overall during the formation of nanoparticles. Even though similar globular proteins are used, the resulting nanoparticles can vary greatly depending on the specific conditions of formation. Understanding these differences can be important for the design and optimization of protein-based nanomaterials for various applications.

3.4.3. *Surface hydrophobicity (H_0) assay*

To further evaluate the structural changes that occur during the NP formation process, we used the ANS assay to determine the surface hydrophobicity of the LV isolate and LV-NPs. The results (Fig. 5) showed that the surfaces of the LV-NPs were slightly less hydrophobic (~5 × 10^6) than the raw material LV isolate (~7 × 10^6), which is consistent with the association of the hydrophilic tri-block copolymer P188 at the surface of the LV-NPs.

3.4.4. *Proposed mechanism of formation of LV-NPs from LV*

The formation of the LV-NPs is proposed to occur as follows (Scheme 3). First, heat treatment (i.e., 80 °C, 20 min) results in a higher degree of protein denaturation, enabling a higher conversion of β-sheets to a more disordered structures, which is consistent with the CD data (Fig. 4). Heating exposes more hydrophobic residues originally in the core of a protein, which facilitates intermolecular aggregation and a reduction of the solution concentration. These exposed hydrophobic residues can associate more freely with the hydrophobic block of the stabilizer P188 to form a hydrophobic core through a supramolecular self-assembly process [45]. The hydrophilic blocks extend into the aqueous solution

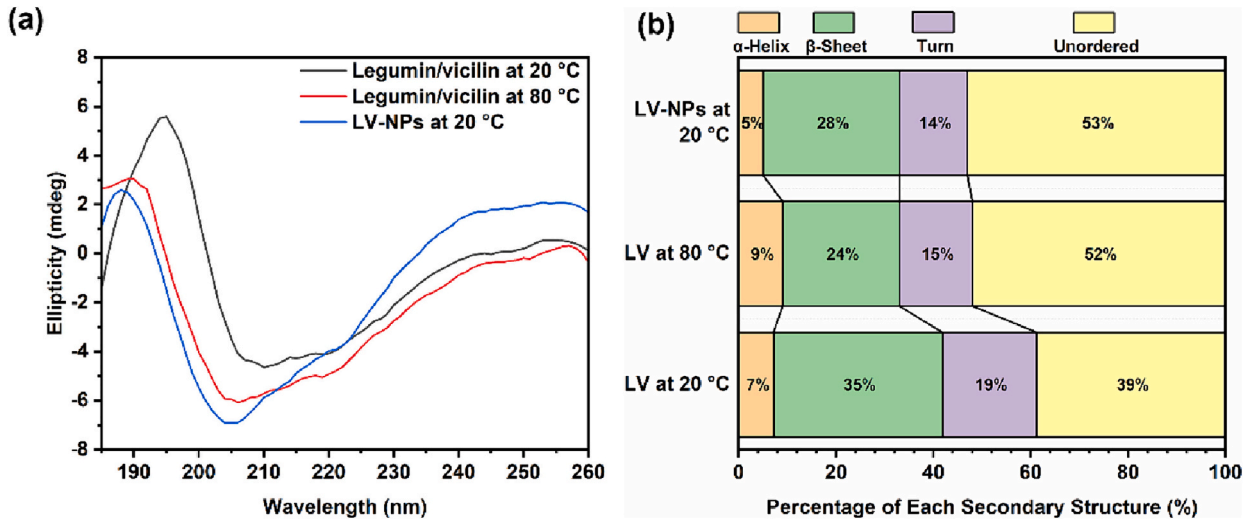

Fig. 4. CD spectra (a) of LV isolate at different temperatures and LV-NPs at 20 °C. (b) is the processed data by DichroWeb, showing percentages of different secondary structures involved in the samples.

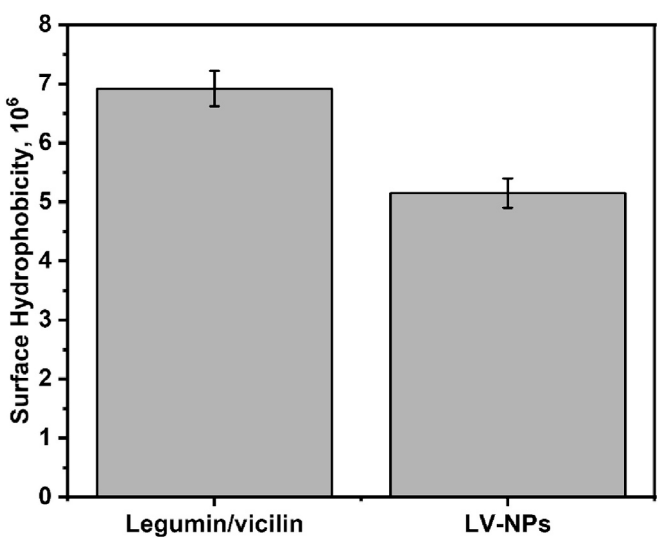

Fig. 5. Surface hydrophobicity assay of legumin/vicilin and LV-NPs.

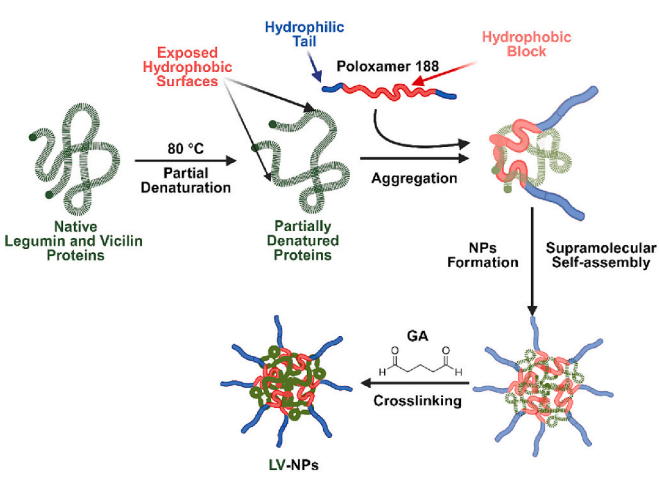

Scheme 3. Proposed self-assembly of LV NPs. GA = glutaraldehyde.

forming a hydrophilic corona, which provides steric stabilization against further interparticle association. Cross-linking of the side chain amine groups of the lysine residues at the hydrophobic/hydrophilic interface with glutaraldehyde irreversibly locks the associated protein structure into place [36]. The resulting NPs have a pseudo-core-shell structure in which the proteins at the interface of the hydrophobic and hydrophilic regions are cross-linked.

3.5. Encapsulation and release of FA from FA-LV-NPs

For FA-encapsulated NPs (FA-LV-NPs), the average D_h was also 50–60 nm, similar to LV-NPs (Fig. S3). The results here confirmed that FA did not have a significant effect on the final particle size or the particle size distribution at a starting FA concentration of 1 mg/mL during the initial loading.

Fluorescence spectroscopy was applied to evaluate the incorporation of FA into the NPs. For these experiments, FA-LV-NPs were synthesized using a constant amount of protein isolate (i.e., 15 mg), while the FA concentration was kept at 1 mg/mL (Scheme 2) during the initial loading. Fluorescence spectra were then recorded on the FA-LV-NPs dispersed in 1× PBS after purification at excitation wavelengths corresponding to the LV-NPs (λ_{ex} = 284 nm) and FA (λ_{ex} = 347 nm) (Fig. 6). While the loading of FA did not significantly affect the intrinsic protein fluorescence signal (Fig. 6a), the fluorescence for FA did increase almost two-fold with starting FA concentration of 1 mg/mL during the initial loading, which suggests the encapsulation of FA in the FA-LV-NPs. In addition, the strong emission signal for FA at ~440 nm (Fig. S4) [46] also red-shifted by 6 nm, which is consistent with the formation of J-aggregates. This result may suggest that the encapsulated FA molecules aggregate while bound to the LV-NPs. Overall, these results suggest that the incorporation of FA during the FA-LV-NP synthesis results in successful loading of FA without a significant effect on the size of FA-LV-NPs.

The release of FA from FA-LV-NPs was carried out in four different types of media to simulate the environments of the stomach and intestines; i.e. SGF (pH = 1.2) with and without the enzyme pepsin and SIF (pH = 6.8) with and without the enzyme pancreatin. The release of FA was higher in SGF compared to SIF, regardless of whether or not enzymes were present. However, the release of FA was higher and faster under both conditions with the enzymes present. Approximately 84 % and 46 % of FA was released during the first 30 min in SGF with and without enzymes, respectively (Fig. 7). In contrast, FA was only released after 30 min. in SIF with the enzyme (~8 %). The release of more FA in

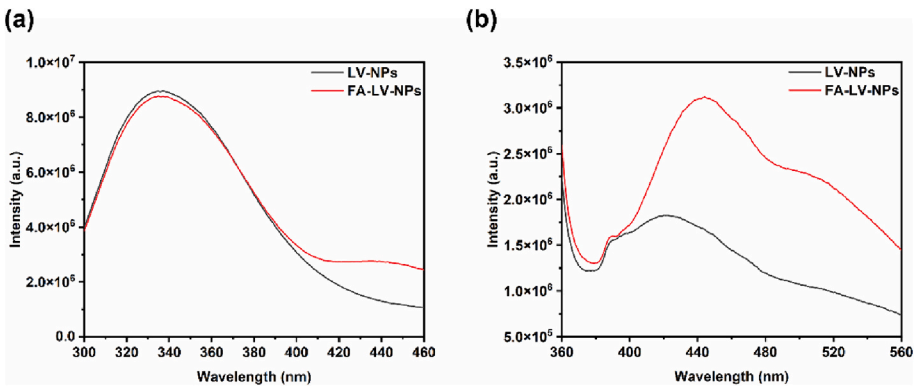

Fig. 6. Effect of FA encapsulation on the fluorescence properties of particles. The samples are dissolved in 1× PBS at a particle concentration of 1 mg/mL. (a) protein intrinsic fluorescence (λ_{ex} = 284 nm) and (b) FA fluorescence (λ_{ex} = 347 nm).

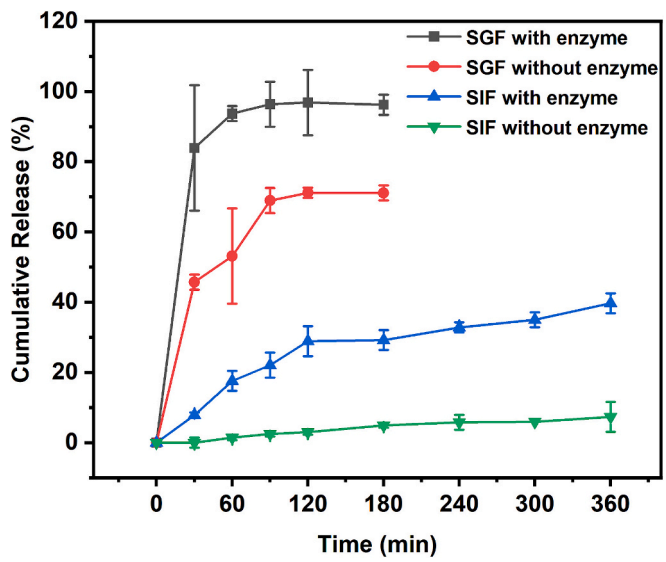

Fig. 7. Release of FA from FA-LV-NPs under different simulated conditions. SGF = simulated gastric fluid. SIF = simulated intestinal fluid.

shorter time in SGF may be due the highly acidic environment, which could facilitate the acid-catalyzed hydrolysis of the dynamic covalent imine bonds, cross-linking the protein backbone [47], enabling less encumbered diffusion of the FA cargo into the surrounding environment. In addition, the more acidic conditions of SGF should weaken FA binding via hydrogen bonding, due to protonation of hydrogen bond acceptor groups on the protein backbone [48]. In contrast, the near neutral pH of SIF favors stronger hydrogen bonding interactions between FA and the protein backbone [49]. The higher release of FA in the presence of the enzymes pepsin and pancreatin is expected and is likely attributed to enzyme induced protein degradation, since both enzymes function to digest proteins in the stomach and intestines, respectively. Overall, the results here showed that FA can be released under different conditions with different release profiles. Furthermore, the findings presented here hold promise for potential applications in in vivo studies, aligning with existing literature [12]. Given the nanoparticle-based nature of our formulation, it can offer advantages over alternative approaches such as tablet supplementation and food fortification. Nanoparticles have demonstrated enhanced oral bioavailability attributed to increased cellular uptake efficiency and targeted delivery capabilities [3], showing the potential superiority of our system.

Compared to other FA delivery systems using food protein-based nanoparticles [12,50], which typically demonstrated higher release in SIF due to low solubility of FA in SGF, our system demonstrates significant divergence. Notably, contrary to previous findings indicating decreased release in SGF due to FA's limited solubility at lower pH, our system exhibits heightened release in this environment, suggesting potential broader applications where improved solubility or augmented delivery in low pH environments, such as the stomach's acidic milieu, is desirable. This feature could prove advantageous in the design of release systems for various drugs, such as the anticancer agent doxorubicin, to achieve targeted release for gastric cancer treatment, or for antibiotics targeting gastric *Helicobacter pylori* infection.

3.6. *In vitro cell viability assay*

In order to determine if the LV-NPs are suitable for biological applications, the cytotoxicity of the nanoparticles on Caco-2 cells was assessed using the alamarBlue assay which measures cell metabolic activity. Caco-2 cells were incubated with different concentrations (0, 0.5, 1, 2 mg/mL) of LV isolate, LV-NPs, and FA-LV-NPs for 24 h and 96 h. At the end of the incubation periods, the reduction of resazurin to resorufin was measured as an indicator of cellular metabolic activity. As shown in Fig. 8, the cells treated with samples were more metabolically active than the control, untreated cells, even after long-term treatment (96 h) at high concentrations of NPs (2 mg/mL). The results suggest that the LV isolate, LV-NPs and FA-LV-NPs did not affect Caco-2 cell metabolic activity, and by extension viability, which suggests that these materials are likely biocompatible. Interestingly, the cells incubated with all three materials show higher cell metabolic activity (>100 %) compared to cells without any treatment, which is expected as proteins are digested into amino acids, which can support some metabolic processes including cell growth. Overall, the results here showed that our materials may be suitable as food additives in the food industry (i.e., nutrient supplements and drug delivery etc.).

4. Conclusions

In summary, protein isolates (i.e., LV) were successfully isolated from commercial fava beans and converted to sterically stabilized, glutaraldehyde cross-linked NPs. The process was carried out successfully both with or without FA to give empty (LV-NPs) or FA-loaded NPs (FA-LV-NPs), without affecting the NP size (~50 nm) or pseudo-spherical morphology. Spectroscopic analysis confirmed that the surfactant P188 was incorporated into the LV-NPs and that the composition of β-structures decreased while disordered structures increased for the LV-NPs relative to the LV isolates. For the FA-LV-NPs, the encapsulation efficiency was 13.5 ± 1.4 % and the loading capacity was 26.3 ± 2.8 mg/g. The rate and total amount of FA released was sensitive to different conditions (i.e., media) such pH and/or the presence/absence of enzymes. Finally, cytotoxicity studies confirmed that Caco-2 cell viability is unaffected by these materials and that they are safe for use for further

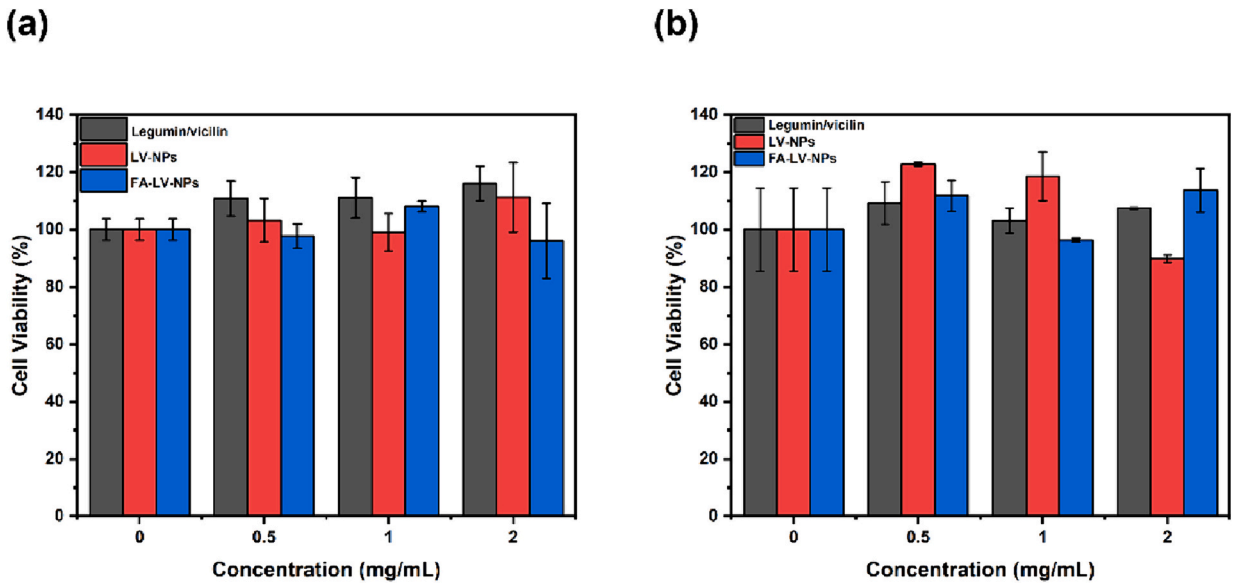

Fig. 8. Caco-2 cell viability after exposure to LV isolate, LV-NPs and FA loaded LV-NPs after (a) 24 h and (b) 96 h. All the data bars were obtained by averaging measurements obtained from 3 different Caco-2 cell cultures, while the error bars indicate the standard deviation.

biological study. This work is expected to further the development of LV protein based functional nanomaterials toward nanocarriers for the delivery of specific pharmaceuticals, bioactives or nutraceuticals.

CRediT authorship contribution statement

Changhao Fang: Writing – original draft, Validation, Methodology, Investigation, Formal analysis, Conceptualization. **Karen Kanemaru:** Investigation. **Wildemar S.P. Carvalho:** Investigation. **Krista R. Fruehauf:** Methodology, Investigation. **Sunshine Zhang:** Investigation. **Prem P. Das:** Validation, Methodology, Investigation, Formal analysis. **Caishuang Xu:** Validation, Methodology, Investigation, Formal analysis. **Yuping Lu:** Validation, Methodology, Investigation, Formal analysis. **Nandhakishore Rajagopalan:** Writing – original draft, Validation, Methodology, Investigation, Formal analysis. **Marianna Kulka:** Writing – review & editing, Supervision, Resources, Project administration, Methodology, Funding acquisition, Conceptualization. **Darren A. Makeiff:** Writing – review & editing, Writing – original draft, Resources, Project administration, Methodology, Funding acquisition, Conceptualization. **Michael J. Serpe:** Writing – review & editing, Supervision, Resources, Project administration, Methodology, Funding acquisition, Conceptualization.

Declaration of competing interest

The authors declare that they have no known competing financial interests or personal relationships that could have appeared to influence the work reported in this paper.

Acknowledgments

The authors gratefully acknowledge support from the Sustainable Protein Production Program of the National Research Council Canada (SPP008-A1-019277). The protein structure graphics were obtained from Protein Data Bank, legumin (3KSC): doi:https://doi.org/10.2210/pdb3KSC/pdb [51]. Vicilin (7U1I): doi:https://doi.org/10.2210/pdb7U1I/pdb [52].

Appendix A. Supplementary data

Supplementary data to this article can be found online at https://doi.org/10.1016/j.ijbiomac.2024.131646.

References

[1] A.R. Singh, P.K. Desu, R.K. Nakkala, V. Kondi, S. Devi, M.S. Alam, H. Hamid, R. B. Athawale, P. Kesharwani, Nanotechnology-based approaches applied to nutraceuticals, Drug Deliv. Transl. Res. (2021) 1–15.
[2] A. Rezaei, M. Fathi, S.M. Jafari, Nanoencapsulation of hydrophobic and low-soluble food bioactive compounds within different nanocarriers, Food Hydrocoll. 88 (2019) 146–162.
[3] T. Zhang, L. Li, S. Chunta, W. Wu, Z. Chen, Y. Lu, Enhanced oral bioavailability from food protein nanoparticles: a mini review, J. Control. Release 354 (2023) 146–154.
[4] L. Rashidi, Different nano-delivery systems for delivery of nutraceuticals, Food Biosci. 43 (2021) 101258.
[5] N. Wald, M. Law, J. Morris, D. Wald, Quantifying the effect of folic acid, Lancet 358 (9298) (2001) 2069–2073.
[6] N.G. Clark, N.F. Sheard, J.F. Kelleher, Treatment of iron-deficiency anemia complicated by scurvy and folic acid deficiency, Nutr. Rev. 50 (5) (1992) 134.
[7] I.I. Kruman, T. Kumaravel, A. Lohani, W.A. Pedersen, R.G. Cutler, Y. Kruman, N. Haughey, J. Lee, M. Evans, M.P. Mattson, Folic acid deficiency and homocysteine impair DNA repair in hippocampal neurons and sensitize them to amyloid toxicity in experimental models of Alzheimer's disease, J. Neurosci. 22 (5) (2002) 1752–1762.
[8] S.J. Duthie, Folic acid deficiency and cancer: mechanisms of DNA instability, Br. Med. Bull. 55 (3) (1999) 578–592.
[9] K.S. Crider, L.B. Bailey, R.J. Berry, Folic acid food fortification—its history, effect, concerns, and future directions, Nutrients 3 (3) (2011) 370–384.
[10] A.M. Gazzali, M. Lobry, L. Colombeau, S. Acherar, H. Azaïs, S. Mordon, P. Arnoux, F. Baros, R. Vanderesse, C. Frochot, Stability of folic acid under several parameters, Eur. J. Pharm. Sci. 93 (2016) 419–430.
[11] Y. Premjit, S. Pandey, J. Mitra, Recent trends in folic acid (vitamin B9) encapsulation, controlled release, and mathematical modelling, Food Rev. Intl. (2022) 1–35.
[12] R. Penalva, I. Esparza, M. Agüeros, C.J. Gonzalez-Navarro, C. Gonzalez-Ferrero, J. M. Irache, Casein nanoparticles as carriers for the oral delivery of folic acid, Food Hydrocoll. 44 (2015) 399–406, https://doi.org/10.1016/j.foodhyd.2014.10.004.
[13] J.A. do Evangelho, R.L. Crizel, F.C. Chaves, L. Prietto, V.Z. Pinto, M.Z. de Miranda, A.R.G. Dias, E. da Rosa Zavareze, Thermal and irradiation resistance of folic acid encapsulated in zein ultrafine fibers or nanocapsules produced by electrospinning and electrospraying, Food Res. Int. 124 (2019) 137–146.
[14] E. Assadpour, Y. Maghsoudlou, S.M. Jafari, M. Ghorbani, M. Aalami, Optimization of folic acid nano-emulsification and encapsulation by maltodextrin-whey protein double emulsions, Int. J. Biol. Macromol. 86 (2016) 197–207, https://doi.org/10.1016/j.ijbiomac.2016.01.064.
[15] X. Ding, P. Yao, Soy protein/soy polysaccharide complex nanogels: folic acid loading, protection, and controlled delivery, Langmuir 29 (27) (2013) 8636–8644, https://doi.org/10.1021/la401664y.
[16] M. Ruiz-Rico, E. Perez-Esteve, M.J. Lerma-Garcia, M.D. Marcos, R. Martinez-Manez, J.M. Barat, Protection of folic acid through encapsulation in mesoporous silica particles included in fruit juices, Food Chem. 218 (2017) 471–478, https://doi.org/10.1016/j.foodchem.2016.09.097.

[17] A. Jain, S.K. Singh, S.K. Arya, S.C. Kundu, S. Kapoor, Protein nanoparticles: promising platforms for drug delivery applications, ACS Biomater Sci. Eng. 4 (12) (2018) 3939–3961, https://doi.org/10.1021/acsbiomaterials.8b01098.
[18] M. Fathi, F. Donsi, D.J. McClements, Protein-based delivery systems for the nanoencapsulation of food ingredients, Comprehensive Reviews in Food Science and Food Safety 17 (4) (2018) 920–936, https://doi.org/10.1111/1541-4337.12360.
[19] Q. Guo, I. Bayram, W. Zhang, J. Su, X. Shu, F. Yuan, L. Mao, Y. Gao, Fabrication and characterization of curcumin-loaded pea protein isolate-surfactant complexes at neutral pH, Food Hydrocoll. 111 (2021), https://doi.org/10.1016/j.foodhyd.2020.106214.
[20] A.G.A. Sá, Y.M.F. Moreno, B.A.M. Carciofi, Plant proteins as high-quality nutritional source for human diet, Trends Food Sci. Technol. 97 (2020) 170–184.
[21] S.S. Nielsen, S.S. Deshpande, M.A. Hermodson, M.P. Scott, Comparative digestibility of legume storage proteins, J. Agric. Food Chem. 36 (5) (1988) 896–902.
[22] K. Schwenke, Reflections about the functional potential of legume proteins: a review, Food/Nahrung 45 (6) (2001) 377–381.
[23] S. Multari, D. Stewart, W.R. Russell, Potential of fava bean as future protein supply to partially replace meat intake in the human diet, Compr. Rev. Food Sci. Food Saf. 14 (5) (2015) 511–522.
[24] D.J. Wright, D. Boulter, Purification and subunit structure of legumin of Vicia faba L.(broad bean), Biochem. J. 141 (2) (1974) 413–418.
[25] A.O. Warsame, N. Michael, D.M. O'Sullivan, P. Tosi, Identification and quantification of major Faba bean seed proteins, J. Agric. Food Chem. 68 (32) (2020) 8535–8544, https://doi.org/10.1021/acs.jafc.0c02927.
[26] J.M. Irache, L. Bergougnoux, I. Ezpeleta, J. Gueguen, A.-M. Orecchioni, Optimization and in vitro stability of legumin nanoparticles obtained by a coacervation method, Int. J. Pharm. 126 (1–2) (1995) 103–109.
[27] I. Ezpeleta, J.M. Irache, S. Stainmesse, C. Chabenat, J. Gueguen, A.-M. Orecchioni, Preparation of lectin-vicilin nanoparticle conjugates using the carbodiimide coupling technique, Int. J. Pharm. 142 (2) (1996) 227–233.
[28] I. Ezpeleta, J. Rache, J. Gueguen, A. Orecchioni, Properties of glutaraldehyde cross-linked vicilin nano-and microparticles, J. Microencapsul. 14 (5) (1997) 557–565.
[29] S.M.T. Gharibzahedi, B. Smith, Legume proteins are smart carriers to encapsulate hydrophilic and hydrophobic bioactive compounds and probiotic bacteria: a review, Comprehensive Reviews in Food Science and Food Safety 20 (2) (2021) 1250–1279.
[30] Y. Fan, X. Zeng, J. Yi, Y. Zhang, Fabrication of pea protein nanoparticles with calcium-induced cross-linking for the stabilization and delivery of antioxidative resveratrol, Int. J. Biol. Macromol. 152 (2020) 189–198, https://doi.org/10.1016/j.ijbiomac.2020.02.248.
[31] H. Zhao, X. Zhou, J. Wang, X. Ma, M. Guo, D. Liu, Heat-induced hollow microcapsule formation using fava bean legumin, Food Hydrocoll. 112 (2021), https://doi.org/10.1016/j.foodhyd.2020.106207.
[32] T. Mirshahi, J.M. Irache, C. Nicolas, M. Mirshahi, J.P. Faure, J. Gueguen, C. Hecquet, A.M. Orecchioni, Adaptive immune responses of legumin nanoparticles, J. Drug Target. 10 (8) (2002) 625–631, https://doi.org/10.1080/1061186021000066237.
[33] L. Whitmore, B. Wallace, DICHROWEB, an online server for protein secondary structure analyses from circular dichroism spectroscopic data, Nucleic Acids Res. 32 (suppl_2) (2004) W668–W673.
[34] C.A. Haskard, E.C. Li-Chan, Hydrophobicity of bovine serum albumin and ovalbumin determined using uncharged (PRODAN) and anionic (ANS-) fluorescent probes, J. Agric. Food Chem. 46 (7) (1998) 2671–2677.
[35] H. Zhao, M. Guo, X. Ma, T. Ding, D. Liu, Microstructure and permeability of hollow microcapsules produced from faba bean 11s protein, Food Hydrocoll. 112 (2021), https://doi.org/10.1016/j.foodhyd.2020.106292.
[36] T. Mirshahi, J.M. Irache, J. Gueguen, A.M. Orecchioni, Development of drug delivery systems from vegetal proteins: legumin nanoparticles, Drug Dev. Ind. Pharm. 22 (8) (2008) 841–846, https://doi.org/10.3109/03639049609065914.
[37] A.D. Hanlon, M.I. Larkin, R.M. Reddick, Free-solution, label-free protein-protein interactions characterized by dynamic light scattering, Biophys. J. 98 (2) (2010) 297–304, https://doi.org/10.1016/j.bpj.2009.09.061.
[38] S. Zhang, J. Li, G. Lykotrafitis, G. Bao, S. Suresh, Size-dependent endocytosis of nanoparticles, Adv. Mater. 21 (4) (2009) 419–424.
[39] M. Jackson, H.H. Mantsch, The use and misuse of FTIR spectroscopy in the determination of protein structure, Crit. Rev. Biochem. Mol. Biol. 30 (2) (1995) 95–120.
[40] S.M. Kelly, N.C. Price, The use of circular dichroism in the investigation of protein structure and function, Curr. Protein Pept. Sci. 1 (4) (2000) 349–384.
[41] F. Husband, P. Wilde, D. Clark, H. Rawel, G. Muschiolik, Foaming properties of modified faba bean protein isolates, Food Hydrocoll. 8 (5) (1994) 455–468.
[42] O. Nivala, E. Nordlund, K. Kruus, D. Ercili-Cura, The effect of heat and transglutaminase treatment on emulsifying and gelling properties of faba bean protein isolate, LWT 139 (2021) 110517.
[43] X.L. Li, Q.T. Xie, W.J. Liu, B.C. Xu, B. Zhang, Self-assembled pea protein isolate nanoparticles with various sizes: explore the formation mechanism, J. Agric. Food Chem. 69 (34) (2021) 9905–9914, https://doi.org/10.1021/acs.jafc.1c02105.
[44] J. Zhang, L. Liang, Z. Tian, L. Chen, M. Subirade, Preparation and in vitro evaluation of calcium-induced soy protein isolate nanoparticles and their formation mechanism study, Food Chem. 133 (2) (2012) 390–399, https://doi.org/10.1016/j.foodchem.2012.01.049.
[45] B.B. Mandal, S.C. Kundu, Self-assembled silk sericin/poloxamer nanoparticles as nanocarriers of hydrophobic and hydrophilic drugs for targeted delivery, Nanotechnology 20 (35) (2009) 355101, https://doi.org/10.1088/0957-4484/20/35/355101.
[46] Hu Wusigale, L., Cheng, H., Gao, Y., & Liang, L., Mechanism for inhibition of folic acid photodecomposition by various antioxidants, J. Agric. Food Chem. 68 (1) (2020) 340–350, https://doi.org/10.1021/acs.jafc.9b06263.
[47] T. Wang, M. Turhan, S. Gunasekaran, Selected properties of pH-sensitive, biodegradable chitosan–poly (vinyl alcohol) hydrogel, Polym. Int. 53 (7) (2004) 911–918.
[48] E. Bottari, A. D'Ambrosio, G. De Tommaso, M.R. Festa, M. Iuliano, M. Meschino, Solubility of folic acid and protonation of folate in NaCl at different concentrations, even in physiological solution, Analyst 146 (7) (2021) 2339–2347.
[49] M.E. Ochnio, J.H. Martinez, M.C. Allievi, M. Palavecino, K.D. Martinez, O.E. Perez, Proteins as Nano-carriers for bioactive compounds. The case of 7S and 11S soy globulins and folic acid complexation, Polymers (Basel) 10 (2) (2018), https://doi.org/10.3390/polym10020149.
[50] P. Zema, A.M. Pilosof, On the binding of folic acid to food proteins performing as vitamin micro/nanocarriers, Food Hydrocoll. 79 (2018) 509–517.
[51] M.R.G. Tandang-Silvas, T. Fukuda, C. Fukuda, K. Prak, C. Cabanos, A. Kimura, T. Itoh, B. Mikami, S. Utsumi, N. Maruyama, Conservation and divergence on plant seed 11S globulins based on crystal structures, Biochimica et Biophysica Acta (BBA)-Proteins and Proteomics 1804 (7) (2010) 1432–1442.
[52] K.A. Robinson, A.D. St-Jacques, I.D. Bakestani, B.A. Beavington, M.C. Loewen, Pea and lentil 7S globulin crystal structures with comparative immunoglobulin epitope mapping, Food Chemistry: Molecular Sciences 5 (2022) 100146.